Drug and Alcohol Dependence 278 (2026) 112972

Contents lists available at ScienceDirect

Drug and Alcohol Dependence

journal homepage: www.elsevier.com/locate/drugalcdep

Acute alcohol intake disrupts resting state network topology in healthy social drinkers

Leah A. Biessenberger [a,*], Adriana K. Cushnie [a], Bethany Stennett-Blackmon [b], Landrew S. Sevel [a], Michael E. Robinson [b], Sara Jo Nixon [c], Jeff Boissoneault [a]

[a] University of Minnesota, Department of Anesthesiology, Minnesota Alcohol and Pain Laboratory, USA
[b] University of Florida, Center for Pain Research and Behavioral Health, USA
[c] University of Florida, Department of Psychiatry, USA

ARTICLE INFO

Keywords:
MRI
Acute alcohol
Graph theory analysis
Network topography
Subjective intoxication

ABSTRACT

Alcohol intake disrupts cognitive and sensory processing. However, its effects on the role of individual structures within cortical networks, or on the larger network structure, remain unclear. This acute alcohol administration study addressed this gap using graph theory analysis. Healthy individuals (n = 107, 21–45 yrs, 61 women) consumed alcohol (0.08 g/dL target BrAC) or a placebo drink in 2 double-blinded sessions and self-reported their perceived intoxication using a visual analog scale. Resting state fMRI was acquired with a Siemens Prisma 3T scanner 30 min after consumption. The effect of alcohol on graph theory outcomes in a network of 106 cerebral ROIs was identified using the CONN toolbox. We also determined the association between graph theory metrics and subjective intoxication. Results revealed alcohol 1) significantly decreased global efficiency in several occipital nodes and increased global efficiency for nodes within the frontal and temporal cortex; 2) increased local efficiency at a network level as well as in specific nodes in the temporal and frontal cortices; 3) increased degree in frontal and temporal regions; 4) decreased closeness centrality and increased mean path length in parietal and occipital regions as well at the network level compared with placebo conditions. Additionally, decreases in global efficiency and increases in local efficiency and clustering coefficient in the alcohol vs. placebo condition significantly predicted subjective intoxication. Taken together, results provide new evidence that alcohol intake produces changes in the overall topography of the cerebral network that at least partially underlie individual differences in subjective alcohol response.

1. Introduction

Approximately half of US adults consume at least 1 alcohol-containing drink per month, with ~2.3 billion people consuming alcohol worldwide (2023 SAMHSA; 2018 Geneva: World Health Organization). Alcohol has profound neurobehavioral effects and chronic heavy use causes significant medical and psychosocial consequences (Boissoneault, 2023). On a synaptic level, acute alcohol consumption increases gamma-aminobutyric acid (GABA) and decreases glutamate transmission in the ventral tegmental area, nucleus accumbens, prefrontal cortex (PFC), and amygdala (Boissoneault, 2023; Roberto, 2003; Basavarajappa et al., 2008). These regions are predominantly associated with reward, aversion, motivation, and executive function. In addition, task-based functional MRI studies indicate alcohol dose-dependently disrupts activation in the anterior cingulate cortex (ACC), dorsolateral PFC (dlPFC), insular cortex, and parietal lobe (regions associated with error processing and cognitive control) during working memory, response inhibition, and set-shifting tasks (Anderson, 2011; Marinkovic, 2012; Paulus, 2006). Although informative, functional activation analyses do not provide information about the broader network or the role a specific region plays within the greater network.

In contrast, resting state functional magnetic resonance imaging (rsfMRI) facilitates assessment of acute alcohol effects on brain networks. The most common approach for analyzing rsfMRI data is to calculate functional connectivity (i.e., correlation strength of the blood oxygen level-dependent (BOLD) time-series) between regions of interest (ROI-to-ROI) or between a single ROI and the rest of the brain (seed-to-voxel). Using this strategy, researchers have identified acute effects of alcohol on functional connectivity of numerous brain regions, including those related to reward, motivation, and salience processing (Han et al.,

* Correspondence to: University of Minnesota, Department of Anesthesiology, B515 Mayo Memorial Building, 420 Delaware St SE, Minneapolis, MN 55455, USA.
E-mail address: biessenb@umn.edu (L.A. Biessenberger).

https://doi.org/10.1016/j.drugalcdep.2025.112972
Received 13 August 2025; Received in revised form 28 October 2025; Accepted 12 November 2025
Available online 22 November 2025

2023; Han, 2021; Shokri-Kojori, 2017; Boissoneault, 2020; Cushnie, 2025; Boissoneault et al., 2020).

Although the effect of acute alcohol on structures and networks underlying inhibitory function, psychomotor performance, and working memory are well described, fewer studies have addressed mechanisms related to subjective alcohol response. Subjective intoxication after alcohol intake is highly variable across individuals, even at the same breath alcohol concentration (BrAC) (Morzorati, 2002; Monds, 2021). In addition, alcohol can have positively or negatively valenced stimulating and sedating effects (Aghabeigi et al., 2024). In previous analyses, greater activity in the nucleus accumbens and left caudate were significantly associated with subjective ratings of intoxication (Gilman, 2008). Gray matter density in the pre-motor cortex and pre-central gyrus is significantly associated with both subjective perceived intoxication and positively-valenced sedation (Stennett-Blackmon et al., 2023).

However, such analyses do not reflect potential changes in the broader structure of functional brain networks, or the role of individual structures within the larger network.

Graph theory-based analysis provides a means of characterizing interconnectivity across a network and is a complementary approach to both functional activation and functional connectivity analyses [for review, see 18]. Graph theory analysis provides novel information regarding alcohol-induced perturbations in network-wide resource use, as well as both global and regional patterns of information processing. In graph theory, ROIs are referred to as nodes and functional connections between nodes are referred to as edges. The brain requires resource management because metabolic resources necessary for information processing and transfer are limited. Restriction of the number of possible edges between nodes, such that clusters of nodes predominantly connect within the cluster and link to other clusters through a centralized node, is thought to reflect this resource management. The cerebral network is thought to exist on a continuum between a fully 'grid-like' state, in which subnetworks communicate only through central hubs, and a 'random' network, where each node is equally likely to have an edge with all nodes (Bullmore and Sporns, 2009). In other words, the most communication occurs between the nodes within a cluster and the chances of interacting with nodes outside that cluster are low save for the low proportion of key nodes with high *clustering coefficients* that transfer information across clusters (Meunier, 2009; Ferrarini, 2009).

Clustering coefficients reflect the connectedness of a node to its nearest node neighbors through a central node. Clusters can act as functional modules, allowing independent and parallel cognitive processing of internal and external informational cues (Laughlin and Sejnowski, 2003; Salinas and Sejnowski, 2001). It is generally accepted that this organization reduces resource requirements for parallel information processing across smaller and larger scale networks in a hierarchical fashion (Achard and Bullmore, 2007; Sporns and Betzel, 2016). In the context of graph theory, this is reflected in measures of *global* and *local efficiency*. *Efficiency* reflects the connectedness (i.e., centrality) of an individual node with either the entire graph (*global*) or its neighboring nodes (*local*). A greater efficiency value is interpreted as a shorter path length between a node and any other node in the graph (global) or between individual nodes with shared edges (local). Theoretically, a shorter path length implies communication between nodes would require fewer resources (Bullmore and Sporns, 2009; Sporns, 2018). Global and local efficiency can also be evaluated at the network level, with network global efficiency reflecting the interconnectedness of all nodes with every other node in the graph and network local efficiency reflecting the local integration of all nodes within the network.

While graph theory analysis has been used to evaluate brain function across multiple tasks and conditions, it has been rarely applied in alcohol-related research. Of the few existing studies, most have focused on the consequences of long-term heavy alcohol use. One such study comparing individuals diagnosed with alcohol use disorder (AUD) and community-dwelling individuals that regularly consume lower quantities of alcohol found lower global and local efficiency in the whole brain, somato-motor, and default mode networks in the AUD group (Lee, 2023). Another comparable study found that a longer history of AUD reduced *degree* (number of edges) and *clustering coefficient* (probability that nodes within the graph will cluster together) in the whole brain network and in nodes associated with cognition and motor control. Clustering coefficients reflect the small-world property of a network (Watts and Strogatz, 1998). Loss of small-world properties (a lower clustering coefficient) is related to poorer results on tests of cognitive performance (Yeung, 2021; Masuda, 2018). The clustering around a core node (related to modularity) reflects degree of interconnectedness at a more localized region (i.e. occipital cortex) as well as the relevance of information flow through a specific node within the greater network structure (Masuda, 2018; Radicchi, 2004; Garcia-Ramos, 2016). Taken together, these studies suggest that a history of chronic heavy alcohol use negatively impacts the topology of brain networks. However, the effect of acute bouts of alcohol consumption on network topology is less clear.

To our knowledge, only one other study has explored the effects of acute alcohol intake on network topology. Zhang et al. (Zhang, 2022) studied the effects of an oral alcohol dose (0.65 g/kg) on resting-state network topology in college-aged individuals without a history of problematic alcohol use, finding that acute alcohol intake significantly altered global efficiency, local efficiency, and clustering coefficient across a range of sparsity values both at the network level and for individual nodes (Zhang, 2022). Although informative, limitations and caveats regarding aspects of the study design and analytical approach suggested the need for additional research. These include the lack of placebo control, the use of a set alcohol dose and post-hoc grouping of participants into 'high' and 'low' BrAC groups, and relatively small sample size. In addition, the association of alcohol-induced changes in network topology with subjective response was not examined.

The current study addressed these limitations, providing novel data regarding the effects of alcohol on network topography through the recruitment of a larger sample ($n = 107$) and use of a within-subject, placebo-controlled design. We used an individually calibrated alcohol dosing paradigm with a BrAC target of 0.08 g/dL, which is associated with significant neurobehavioral impairment. We hypothesized that alcohol administration would perturb the topological structure of cerebral networks in a nuanced manner. We expected that ROIs previously reported to be disrupted by alcohol would emerge as significant nodes, including the insular cortex, nucleus accumbens, and premotor cortex. However, we expected these effects would differ between nodes, as opposed to broad increases or decreases. Additionally, we predicted that the effects of alcohol on network topography would be significantly associated with subjective alcohol response.

2. Materials and methods

2.1. Participants

Community-dwelling healthy individuals ($n = 107$; 26 ± 4 years; 57 % self-identified as women) from north central Florida were included in this secondary analysis of a larger study examining biopsychosocial mechanisms underlying alcohol analgesia (NIH: R01AA025337; ClinicalTrials.gov #NCT04925076). All participants provided informed consent. The University of Florida IRB approved the study.

2.2. Screening

Participants provided demographics, medical history, and completed a series of psychological questionnaires (Beck Depression Inventory II (Yeung, 2021), State-Trait Anxiety Inventory (Masuda, 2018), Alcohol Use Questionnaire (Radicchi, 2004), and Alcohol Use Disorder Identification Test (Garcia-Ramos, 2016). The exclusionary criteria were: consuming < 1 alcohol-containing beverage/month during the prior 6 months; being alcohol naïve, history of drug or alcohol dependence,

problematic alcohol use (AUDIT≥8), past or current chronic pain; regular use of pain-relieving medications; self-reported mild cognitive impairment; psychotic disorders; under-controlled hypertension or diabetes; neurological disease; serious medical illness; and lifetime smoking > 100 cigarettes. Participants were permitted prescription and over-the-counter (OTC) medication that did not contraindicate alcohol intake.

2.3. Study design

Participants completed 2 double-blinded sessions at least 48 h apart. Participants were instructed to fast for 4 hrs and abstain from consuming alcohol for 24 hrs prior to each session. Medications were permitted except for allergy medications or analgesics on the day of testing. Participants also provided a urine sample for drug (THC, cocaine, benzodiazepines, morphine, and methamphetamine) and pregnancy testing at each session. Finally, a breathalyzer was used and participants with a positive breath alcohol concentration (BrAC) were excluded. Participants were provided and consumed a ~220–250 kcal breakfast 1 hr prior to alcohol administration.

The alcohol and placebo sessions were counterbalanced across participants. In each session, participants were given a placebo (0.00 g/dL target BrAC) or alcohol-containing beverage (0.08 g/dL target BrAC). The quantity of the administered alcohol (95 % medical-grade ethanol) needed to achieve.08 g/dL was calculated with the Widmark equation (Zhang, 2022) and the ethanol was mixed with sugar-free lemon-lime soda (1:3 ratio). All drinks were misted with ethanol, and a small amount of ethanol was placed on the surface and rim of placebo beverages to mask the study condition. Participants consumed both beverages ≤ min and rinsed their mouths thoroughly with water afterwards.

2.4. Breath and saliva alcohol concentration

After beverage administration, BrAC was measured every 10 min with a breathalyzer (CMI, Inc., Owensboro, KY). After being positioned in the scanner bore, salivary alcohol concentration (SAC) was assessed between specific testing (QED A150 tests, OraSure Technologies, Inc., Bethlehem, PA). BrAC measures were resumed after removal from the MRI. Participants returned home via HIPAA-compliant rideshare service once their BrAC was ≤ 0.02 g/dL.

2.5. Subjective intoxication and valenced arousal responses

Immediately before resting state fMRI acquisition, participants rated their subjective intoxication (from “not intoxicated” to “most intoxicated imaginable”) using an electronic 0–100 visual analog scale (VAS; (Morean et al., 2013) and completed the subjective effects of alcohol scale [SEAS; 33]. The SEAS captures four domains of subjective responses after drinking alcohol vs. placebo: low-arousal positive (Low+; relaxed, secure, calm, mellow), high-arousal positive (High+; lively, fun, funny, talkative), low-arousal negative (Low-; wobbly, woozy, dizzy), and high arousal negative (High-; rude, aggressive, demanding). Items comprising the High+ , Low+ , High-, and Low- domains were averaged for analysis.

2.6. MRI data acquisition

A Siemens Prisma 3T scanner with a 64-channel head coil was used to collect the imaging data. Participants were placed into the scanner ~25–30 min after consuming the alcohol or placebo beverage. Approximately 5 min later, a 9-minute eyes-open, resting state functional scan was collected with parameters: field-of-view (FOV) = 240 mm, voxel-wise resolution = 2.5 × 2.5 × 2.5 mm, 51 axial slices, inter-slice gap = 0, acceleration factor = 3, and TR/TE/FA = 1500 ms/30 ms/70°. Participants were instructed to keep their gaze on a fixation cross, let their thoughts wander, keep as still as possible, and stay awake. A T1-weighted whole-brain structural image was also acquired, with parameters: FOV = 256 mm, voxel-wise resolution= 0.8 × 0.8 × 0.8 mm, 320 contiguous sagittal slices, acceleration factor = 2, and TR/TE/ FA= 2000 ms/2.99 ms/8°.

2.7. Image processing and analysis

Preprocessing of the fMRI data was completed with SPM12 (Welcome Trust Centre for Neuroimaging, London, UK) and the CONN toolbox v18b (Menardi et al., 2024). Pre-processing included slice-time correction, realignment, registration, normalization to MNI space, spatial smoothing (8 mm FWHM kernel), and motion and signal artifact reduction using the Artifact Detection Toolbox (ART; http://www.nitrc.org/projects/artifact_detect). Outliers were identified as volumes where change in mean global signal exceeded 3 standard deviations, translation exceeded 0.5 mm, or rotation exceeded 0.02 rad from the previous image (Alba-Ferrara, 2016). Component-based noise correction for physiological and other noise source reduction was applied during first-level processing (CONN toolbox default) (Visontay, 2022). Regression analysis was used to reduce the influence of 5 principal components each from signal within CSF and deep cerebral white matter, all six movement parameters and their first-order derivatives, and ART-designated outlier volumes. Mean framewise displacement did not differ significantly between the alcohol and placebo conditions (t_{106}=.88, p = .38). Similarly, there was not a significant difference in the mean number of outlier volumes between beverage conditions (t_{106}=1.85, p = .067).

2.8. Graph theory analysis strategy

Graph theory analysis was performed in the CONN Toolbox (conn22v2407, MATLAB 2024b, The Mathworks Inc). The default CONN Toolbox atlas (Harvard-Oxford atlas) was used to identify 106 ROIs extending from the brainstem to encompass all cortical and subcortical structures. The cerebellum was not included given inconsistent inclusion in the field of view across all participants. The cost (k) threshold was set at 0.25 so the graph results remained within the physiologically relevant range of network sparsity (Bullmore and Sporns, 2009). We chose to threshold edges based on cost (vs. raw correlation coefficients) to normalize the number of edges within graphs between individuals. General linear models (GLM) were used to examine changes in graph theory measures (global efficiency, local efficiency, closeness centrality, degree, mean path length, and clustering coefficient) between the placebo and alcohol conditions. We controlled for session order (placebo or alcohol first) as a second-level covariate (Cushnie, 2025). All analyses were FDR-corrected to control for the large number of simultaneous inferences (p_{FDR}<.05) (Sjoerds, 2017).

2.9. Subjective response analysis strategy

Paired t-tests were used to compared subjective intoxication and SEAS ratings between the alcohol and placebo conditions. Finally, we ran additional GLM analyses (p_{FDR}<.05) identifying associations of alcohol-induced changes in graph theory metrics with subjective intoxication and Low+ , High+ , Low-, and High- SEAS scores. As above, GLM analyses controlled for session order.

3. Results

3.1. Participant characteristics and subjective intoxication

Participant outcomes for BrAC at imaging onset, average SAC during the acquisition, self-reported intoxication during both conditions, AUQ, AUDIT, BDI, and STAI are reported in Table 1. There was a significant difference in the self-reporting of perceived intoxication between the alcohol and placebo conditions (alc: 33.5 ± 5.5, plac: 8.1 ± 12.2,

Table 1
Participant characteristics.

Measure	Mean (SD)
Pre-scan BrAC (g/dL)	0.057 (0.021)
Mean SAC (g/dL)	0.077 (0.014)
Subjective Intoxication (Alcohol) (0–100 VAS)	33.5 (5.5)
Subjective Intoxication (Placebo) (0–100 VAS)	8.1 (12.2)
QFI (oz. abs. EtOH/day)	0.47 (0.31)
AUDIT (total score)	4.73 (1.8)
BDI-II (total score)	2.6 (3.1)
STAI (state total score)	25.5 (5.8)

BrAC: Breath alcohol concentration, SAC: salivary alcohol concentration, QFI: quantity-frequency index, AUDIT: Alcohol Use Disorders Identification Test, BDI-II: Beck Depression Inventory, 2nd edition, STAI: State-Trait Anxiety Inventory

Cohen's d=1.71, t = 17.62, $p < 0.01$).

There were significant differences between the alcohol and placebo conditions for High+ (alc: 23.83 ± 9.24, plac: 19.25 ± 8.64, Cohen's d=0.56, t = 5.82, $p < 0.001$), High- (alc: 1.05 ± 2.51, plac: 0.27 ± 1.19, Cohen's d=0.28, t = 2.91, $p = 0.002$) and Low- (alc: 7.78 ± 7.29, plac: 1.67 ± 2.69, Cohen's d=0.89, t = 9.16, $p < 0.001$) for SEAS scores. There was no significant difference between conditions for the Low+ scores (alc: 29.26 ± 7.26, plac: 29.69 ± 1.09, Cohen's d=-0.06, t = -0.65, $p = 0.52$).

3.2. Graph theory measures

Fig. 1 presents an overview of the effects of alcohol on each graph theory measure, with detailed results presented in subsections below.

3.2.1. Global and local efficiency

Global efficiency was significantly decreased for 9 nodes in the visual cortex and increased for the left planum temporale (auditory cortex) and right insular cortex (sensorimotor) for the alcohol compared with placebo condition (Table 2). There was no significant change in the network level for global efficiency. Local efficiency was significantly increased at the network level as well as in temporal and parietal cortices for the alcohol compared with placebo condition (Table 3).

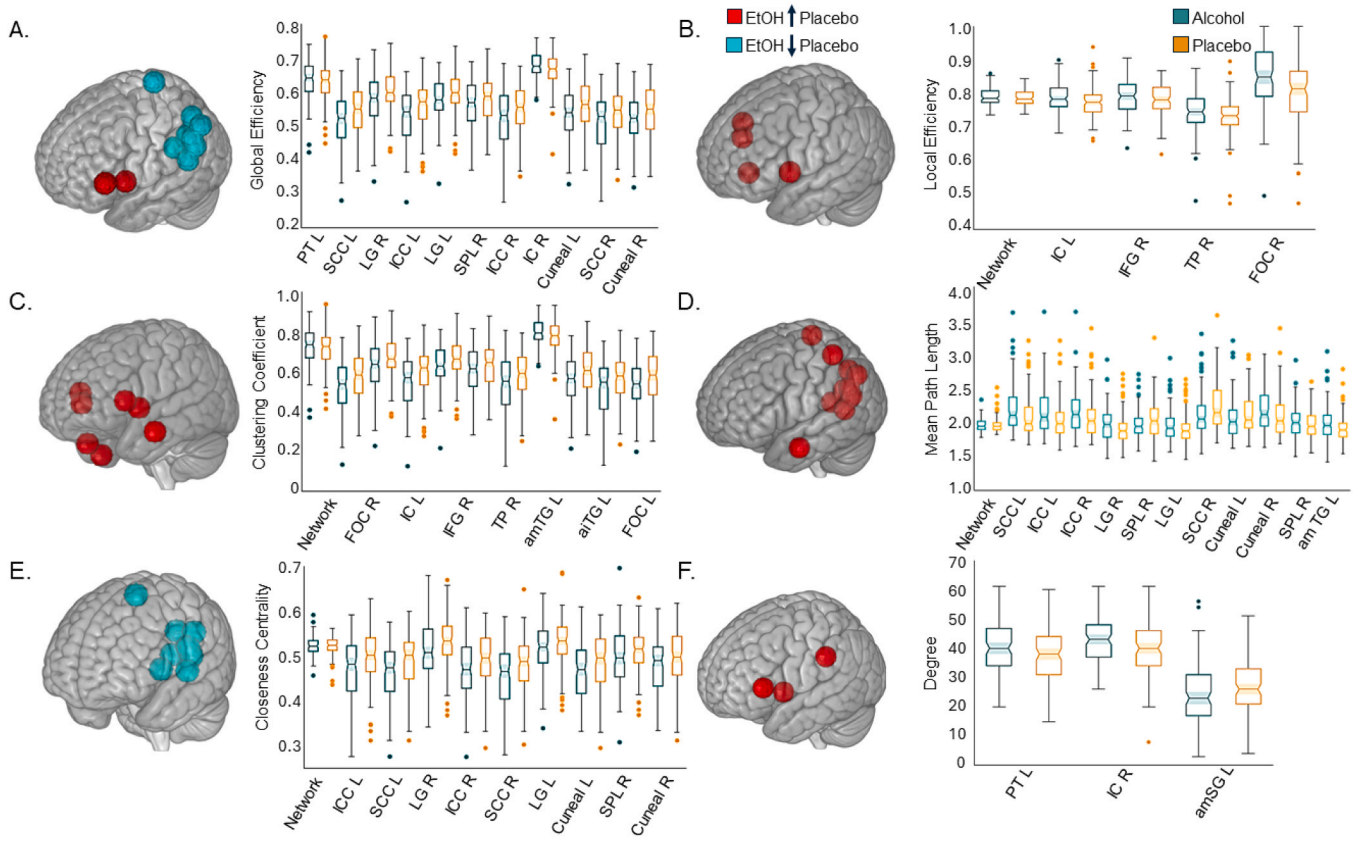

Fig. 1. Significant nodes for each graph theory metric. Each panel contains an image of the brain with significant increases (red) and decreases (blue) by ROI as well as box-and-whisker plots illustrating the effect of alcohol (teal) compared with placebo (gold). **(A) Global efficiency** increased in the PT L and IC R and decreased in SCC L, LG R, ICC L, LG L, SPL R, ICC R, cuneal L, SCC R, and cuneal R. **(B) Local efficiency** increased at the network level as well as in IC L, IFG R, TP R, and FOC R. **(C) Clustering coefficient** increased at the network level as well as in the FOC R, IC L, IFG R, TP R, amTG L, aiTG R, and FOC L. **(D) Mean Path Length** increased at the network-level as well as in the SCC L, ICC L, ICCR, LGR, SPL R, LG L, SCC R, cuneal L, cuneal R, SPL L, and amTG. **(E) Closeness Centrality** decreased at the network level as well as in the ICC L, SCC L, LG R, ICC R, SCC R, LG L, cuneal R, SPL R, and cuneal L. **(F) Degree** increased in PT L, IC R, amSG L. The x-axis for each box-and-whisker plot is arranged from network effect (if significant) as the first on the left of the axis and then the nodes with the strongest to least significance progressing from left to right along the axis. L or R after the node/ROI acronym for the x-axis labels indicates left or right side of the brain. Node/ROI acronyms: anterior inferior temporal gyrus (aiTG), anterior middle temporal gyrus (amTG), anterior supramarginal gyrus (aSMG), frontal operculum cortex (FOC), inferior frontal gyrus (IFG), insular cortex (IC), intracalcarine cortex (ICC), lingual gyrus (LG), planum temporale (PT), supracalcarine cortex (SCC), superior parietal lobule (SPL), temporal pole (TP).

Table 2
GLM results for global efficiency in the alcohol and placebo conditions.

Global Efficiency	EtOH	Placebo	b	p_{FDR}
Planum Temporale L	0.66 ± 0.05	0.65 ± 0.05	0.03	0.012
Supracalcarine Cortex L	0.51 ± 0.08	0.54 ± 0.07	-0.05	0.015
Lingual Gyrus R	0.58 ± 0.07	0.60 ± 0.06	-0.04	0.015
Intracalcarine Cortex L	0.53 ± 0.08	0.56 ± 0.07	-0.04	0.019
Lingual Gyrus L	0.58 ± 0.06	0.60 ± 0.06	-0.03	0.049
Superior Parietal Lobe R	0.56 ± 0.07	0.58 ± 0.06	-0.03	0.049
Intracalcarine Cortex R	0.53 ± 0.08	0.55 ± 0.07	-0.04	0.049
Insular Cortex R	0.68 ± 0.04	0.66 ± 0.05	0.02	0.049
Cuneus L	0.54 ± 0.07	0.56 ± 0.07	-0.03	0.049
Supracalcarine Cortex R	0.51 ± 0.08	0.54 ± 0.07	-0.03	0.049
Cuneus R	0.52 ± 0.08	0.55 ± 0.08	-0.03	0.049

Mean ± sd for global efficiency in the alcohol (EtOH) and placebo conditions, respectively. The nodes are listed in order of significance based on the GLM (coefficient (b) and FDR-corrected *p*-value (p_{FDR})). L and R indicate left or right side of the brain.

3.2.2. Clustering coefficient

Clustering coefficient was significantly increased at the network level as well as in the temporal and parietal cortices in the alcohol compared with placebo condition with the strongest effects in the right frontal operculum cortex, left insular cortex, and right inferior frontal gyrus (Table 4).

Table 3
GLM results for local efficiency in the alcohol and placebo conditions.

Local Efficiency	EtOH	Placebo	beta	pFDR
Network	0.80 ± 0.02	0.79 ± 0.02	0.01	0.02
Insular Cortex L	0.79 ± 0.04	0.77 ± 0.05	0.03	0.01
Inferior Frontal Gyrus R	0.79 ± 0.05	0.78 ± 0.05	0.03	0.01
Temporal Pole R	0.75 ± 0.06	0.74 ± 0.06	0.04	0.01
Frontal Operculum Cortex R	0.85 ± 0.09	0.81 ± 0.09	0.05	0.02

Mean ± sd for local efficiency in the alcohol (EtOH) and placebo conditions, respectively. The nodes are listed in order of significance based on the GLM, (coefficient (b) and FDR-corrected *p*-value (p_{FDR})). L and R indicate left or right side of the brain.

Table 4
GLM results for clustering coefficient in the alcohol vs placebo condition.

Clustering Coefficient	EtOH	Placebo	beta	pFDR
Network	0.62 ± 0.05	0.61 ± 0.05	0.02	0.002
Frontal Operculum Cortex R	0.72 ± 0.15	0.64 ± 0.14	0.09	0.01
Insular Cortex L	0.58 ± 0.09	0.55 ± 0.09	0.05	0.01
Inferior Frontal Gyrus R	0.59 ± 0.10	0.57 ± 0.08	0.05	0.01
Temporal Pole R	.51 ± 0.09	0.49 ± 0.08	0.06	0.01
Anterior Middle Temporal Gyrus L	0.64 ± 0.11	0.59 ± 0.10	0.07	0.01
Anterior Inferior Temporal Gyrus R	0.65 ± 0.15	0.62 ± 0.14	0.07	0.02
Frontal Operculum Cortex L	0.67 ± 0.15	0.63 ± 0.15	0.08	0.03

Mean ± sd for clustering coefficient in the alcohol (EtOH) and placebo conditions, respectively. The nodes are listed in order of significance based on the GLM (coefficient (b) and FDR-corrected *p*-value (p_{FDR})). L and R indicate left or right side of the brain.

Table 5
GLM results for closeness centrality between the alcohol and placebo conditions.

Closeness Centrality	EtOH	Placebo	beta	pFDR
Network	0.52 ± 0.02	0.52 ± 0.02	-0.01	0.04
Intracalcarine Cortex L	0.47 ± 0.06	0.50 ± 0.06	-0.04	0.003
Supracalcarine Cortex L	0.46 ± 0.07	0.49 ± 0.06	-0.05	0.003
Lingual Gyrus R	0.53 ± 0.06	0.51 ± 0.06	-0.04	0.005
Intracalcarine Cortex R	0.47 ± 0.07	0.49 ± 0.06	-0.04	0.005
Supracalcarine Cortex R	0.46 ± 0.06	0.48 ± 0.06	-0.03	0.02
Lingual Gyrus L	0.52 ± 0.06	0.53 ± 0.06	-0.03	0.02
Cuneus R	0.47 ± 0.06	0.48 ± 0.07	-0.03	0.03
Superior Parietal Lobe R	0.50 ± 0.06	0.51 ± 0.05	-0.03	0.03
Cuneus L	0.48 ± 0.06	0.50 ± 0.06	-0.03	0.03

Columns 1 and 2 present the mean ± sd for closeness centrality in the alcohol (EtOH) and placebo conditions, respectively. The nodes are listed in order of significance based on the GLM, for which the coefficient (b) and FDR-corrected *p*-value (p_{FDR}) are reported in columns 3 and 4. L and R indicate left or right.

3.2.3. Closeness centrality

Closeness centrality was significantly decreased at the network level as well as across the occipital cortex, with the most significant effects in the left intracalcarine and supracalcarine cortices and right lingual gyrus progressing to the next lowest orders of significance in the same order on the opposite sides (right intracalcarine and supracalcarine cortices; Table 5).

3.2.4. Mean path length

Alcohol significantly increased mean path length at the network level compared with placebo. In addition, increased mean path length was identified for multiple individual nodes, especially within the occipital cortex. These included left supracalcarine cortex, left and right intracalcarine cortex, and right lingual gyrus (Table 6).

3.2.5. Degree

Degree was significantly increased for 3 nodes for the alcohol compared with placebo condition: left planum temporale, right insular cortex, left anterior middle temporal gyrus (Table 7).

3.3. Subjective reports related to graph theory outcomes

3.3.1. Self-reported intoxication related to graph theory outcomes

Alcohol-induced network-level changes in global efficiency, local efficiency, and clustering coefficient were significantly associated with subjective intoxication (Fig. 2). Global efficiency showed an inverse relationship with alcohol-induced increases in subjective intoxication

Table 6
GLM results for mean path length in the alcohol vs placebo conditions.

Mean Path Length	EtOH	Placebo	beta	pFDR
Network	1.96 ± 0.09	1.96 ± 0.11	0.04	0.02
Supracalcarine Cortex L Cortex L	2.21 ± 0.35	2.09 ± 0.31	0.24	0.005
Intracalcarine Cortex L	2.16 ± 0.33	2.05 ± 0.30	0.19	0.005
Intracalcarine Cortex R	2.17 ± 0.33	2.07 ± 0.30	0.19	0.005
Lingual Gyrus R	1.97 ± 0.24	1.90 ± 0.21	0.15	0.005
Superior Parietal Lobe R	2.03 ± 0.25	1.98 ± 0.19	0.13	0.013
Lingual Gyrus L	1.95 ± 0.23	1.91 ± 0.22	0.13	0.021
Supracalcarine Cortex R	2.23 ± 0.35	2.12 ± 0.31	0.17	0.021
Cuneus L	2.11 ± 0.28	2.04 ± 0.28	0.14	0.021
Cuneus R	2.19 ± 0.31	2.11 ± 0.32	0.15	0.024
Superior Parietal Lobe L	2.02 ± 0.22	1.98 ± 0.20	0.1	0.032
Anterior Middle Temporal Gyrus L	1.99 ± 0.24	1.92 ± 0.11	0.09	0.047

Mean ± sd for mean path length in the alcohol (EtOH) and placebo conditions. The nodes are listed in order of significance based on the GLM (coefficient (b) and FDR-corrected *p*-value (p_{FDR})). L and R indicate left or right side of the brain.

Table 7
GLM results for degree in the alcohol vs placebo conditions.

Degree				
	EtOH	Placebo	beta	pFDR
Planum Temporale L	40.32 ± 8.84	37.51 ± 9.67	6.13	0.0006
Insular Cortex R	42.95 ± 7.36	39.81 ± 9.36	5.18	0.008
Anterior Supramarginal Gyrus L	32.18 ± 9.42	28.23 ± 10.37	5.22	0.043

Mean ± sd for degree in the alcohol (EtOH) and placebo conditions. The nodes are listed in order of significance based on the GLM (coefficient (b) and FDR-corrected *p*-value (p_{FDR})). L and R indicate left or right side of the brain.

(R^2=0.038, *p*FDR=0.01). In contrast, greater network-level local efficiency (R^2=0.061, p_{FDR}=0.002) and clustering coefficient (R^2=0.039, p_{FDR}=0.009) after alcohol intake were associated with increases in intoxication.

3.3.2. SEAS scores related to graph theory outcomes

Alcohol-induced network-level changes in global efficiency (R^2=0.021, p_{FDR}=0.022) and clustering coefficient (R^2=0.02, p_{FDR}=0.043) were significantly associated with Low+ SEAS scores. There were no significant network-level associations for Low-, High+, or High- SEAS scores.

4. Discussion

The present study found that a dose of alcohol targeting a BrAC of 0.08 g/dL significantly altered graph topology at both the network and individual node levels compared to placebo in a cohort of healthy social community-dwelling individuals that regularly consume lower quantities of alcohol drinkers. At the network level, alcohol significantly increased local efficiency and clustering coefficient, consistent with a less random and more grid-like topology. Notably, these increases, as well as corresponding decreases in global efficiency, significantly predicted greater subjective intoxication. In addition, we found that positively-valenced sedating effects of alcohol were significantly associated with global efficiency and clustering coefficient at the network level. Taken together, these findings suggest subjective response to alcohol may be at least partially driven by a shift in the broader brain network towards more regionally isolated information transfer. Previous work has implied that more integrated networks are associated with better executive function, including inhibition of prepotent responses (Menardi et al., 2024). Additionally, network-level efficiency measures are significantly associated with stimulus valence and reward, including in individuals with AUD (Alba-Ferrara, 2016). Therefore, our results that information transfer becomes more isolated and less integrated are consistent with alcohol's known influence on reward/aversion, inhibitory control, and stimulus valence.

We found that acute alcohol intake increased clustering coefficient, mean path length, and local efficiency at the network level and produced

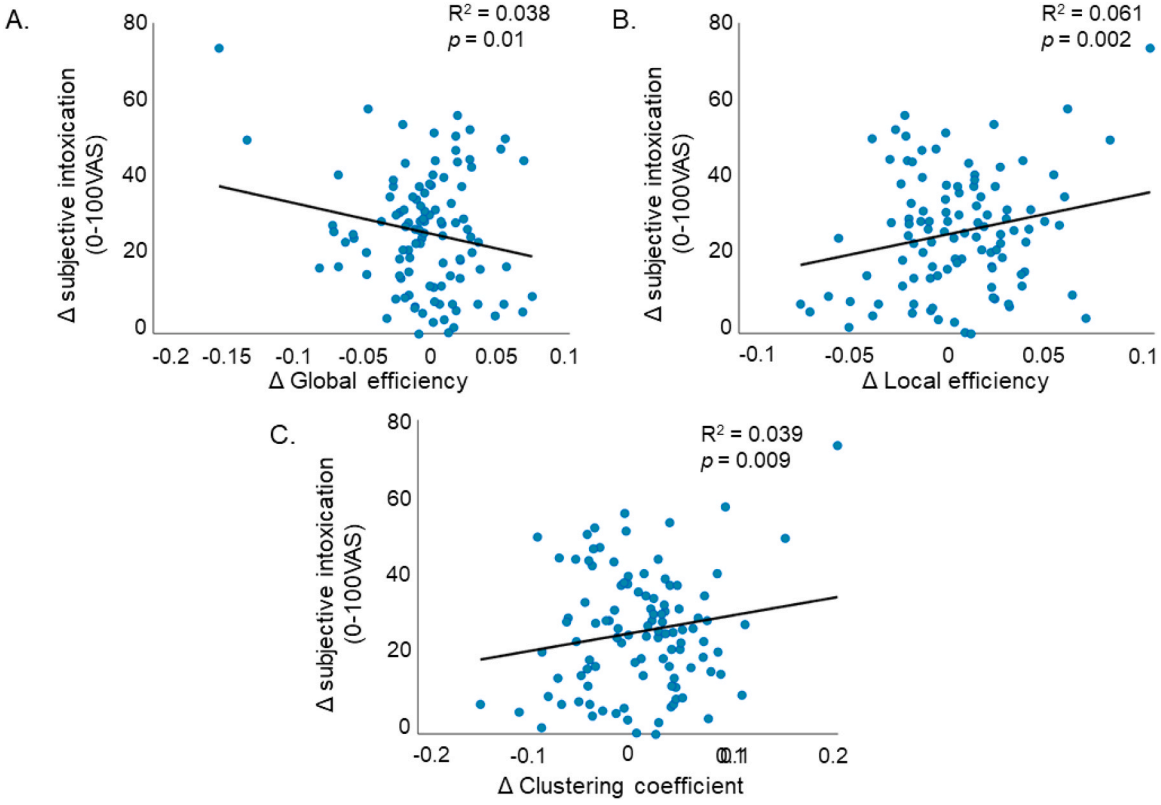

Fig. 2. Between changes in subject intoxication and network-level graph theory metrics. Scatterplots with a trendline for the relation between the difference (Δ) in subjective intoxication and the difference in (A) global efficiency, (B) local efficiency, and (C) clustering coefficient at the network level. Differences were calculated as alcohol – placebo.

complementary changes in graph metrics at multiple specific nodes compared to placebo. However, consistent with evidence that acute and chronic alcohol intake frequently have divergent neurobehavioral effects (Boissoneault, 2023; Visontay, 2022), evidence suggests that chronic heavy alcohol consumption may produce opposite shifts in network topology, consistent with a more random and less grid-like pattern potentially underlying chronic alcohol-induced neurobehavioral compromise. For example, Sjoerds et al. found that heaviness of alcohol use and use duration were associated with reduced clustering coefficient at both the network level and within the caudate nucleus and putamen (Sjoerds, 2017), and Lee et al. identified significant decreases in local efficiency at both the network and regional levels in abstinent AUD individuals compared to controls (Lee, 2023).

Prior investigations have also identified significant acute alcohol effects on network topography, although the directionality of their results differed. In contrast to the present report, Zhang et al. (Zhang, 2022) found that alcohol tended to decrease local efficiency, path length, and clustering coefficient, especially among individuals achieving a relatively higher BrAC. The reason for this discrepancy is unclear, and substantial methodological differences between studies (e.g., sample size, alcohol dosing strategy, MRI methodology, and analytic approach) complicate direct comparison.

Regarding individual nodes, we identified significant changes in global and local efficiency, clustering coefficient, closeness centrality, mean path length, and degree compared with placebo. Broadly, these effects were consistent with the transition to a more grid-like topology observed at the network level noted above. We found that 9 of 11 significant nodes for global efficiency and all nodes for closeness centrality were decreased. In contrast, all significant nodes for mean path length, clustering coefficient, local efficiency, and degree were increased in the alcohol compared with placebo condition. We also found broad disruptions in the parietal lobe and insular cortex that are consistent with a previous report from our lab showing perturbations in insular connectivity with the rest of the brain using seed-to-voxel functional connectivity analysis (Cushnie, 2025). Specifically, alcohol significantly increased global efficiency, local efficiency, and degree of the insular cortex. This reflects increased information transfer of the insula both with the greater network (global efficiency) as well as with adjacent nodes (local efficiency and degree). Also consistent with our hypothesis, alcohol significantly increased local efficiency and clustering coefficient for the inferior frontal gyrus, reflecting increased connectivity and information processing within a localized cluster. Counter to our hypothesis, the nucleus accumbens did not emerge as a significant node for any of the graph theory metrics. This may be because the ventral tegmental area is not included in the Harvard-Oxford atlas implemented in the CONN Toolbox. Release of dopamine from the ventral tegmental area to the nucleus accumbens is important for response to rewarding/aversive stimuli (McCutcheon, 2012; You et al., 2018).

We also noted significant effects of alcohol on brain network topology for multiple nodes within the visual cortex, including decreased global efficiency and closeness centrality and increased mean path length. Significant nodes within the visual cortex included regions associated with both early-stage visual processing such as spatial orientation (i.e., supracalcarine and intracalcarine cortex) and higher-level cognitive processing such as visual memories (i.e., lingual gyrus). Alcohol has well-characterized effects on visual function, including disruption of saccades and smooth pursuit, impaired spatial awareness, and reduced contrast sensitivity (Z.W, 1940; Calhoun, 2004; Roche and King, 2010). Theoretically, decreased global efficiency and closeness centrality for nodes within the occipital cortex may reflect decreased information transfer with the rest of the cerebral network. Similarly, a greater path length implies less efficient use of resources during visual processing, consistent with altered/disrupted visual function after consumption of alcohol. Future studies should investigate whether changes in visual cortex network topology may underlie alcohol-induced impairment in visual function.

4.1. Future directions, strengths, & limitations

In addition, both this study and prior investigations of acute alcohol effects on network topology have included primarily healthy young adults with low-risk drinking patterns and minimal negative affective symptomology (Zhang, 2022). Evidence suggests healthy aging is associated with decreased global and local efficiency in older adults compared with younger adults (Achard and Bullmore, 2007). Given rapid changes in population demographics and increasing rates of drinking among older adults (Han, 2017), studies of the functional neural correlates of acute alcohol use across the lifespan, in populations with heavier drinking patterns, and a broader range of negative affective symptomatology are needed.

The relatively large sample size and use of a double-blind, placebo-controlled design compared with prior investigations of the effect of alcohol on network topology is a significant strength of this study (Zhang, 2022; Sjoerds, 2017). However, cerebellar structures could not be included in our analysis because the cerebellum was inconsistently captured within the field of view during fMRI acquisition. Cerebellar function is disrupted by both acute and chronic alcohol consumption and has extensive reciprocal connections with cortical and subcortical regions (Volkow, 1988; Wang et al., 2025). Therefore, future exploration of the effects of alcohol both within cerebellar topographical networks and the cerebellar nodes related to the broader network is warranted.

4.2. Summary

Taken together, our results suggest that alcohol intake acutely alters the structure of cerebral networks in the resting state, resulting in a more locally clustered and grid-like topology that is less globally integrated. Changes in graph metrics at the network level predicted a moderate but significant amount of the difference in self-reported intoxication between alcohol and placebo conditions, suggesting these effects partially underlie subjective alcohol response.

CRediT authorship contribution statement

Sevel Landrew S: Writing – review & editing, Formal analysis, Conceptualization. **Stennet-Blackmon Bethany:** Writing – review & editing, Data curation. **Cushnie Adriana K:** Writing – review & editing, Validation. **Leah A Biessenberger:** Writing – review & editing, Writing – original draft, Visualization, Validation, Formal analysis. **Jeff Boissoneault:** Writing – review & editing, Writing – original draft, Validation, Supervision, Project administration, Methodology, Investigation, Funding acquisition, Formal analysis, Data curation, Conceptualization. **Sara Jo Nixon:** Writing – review & editing, Conceptualization. **Robinson Michael E E:** Writing – review & editing, Conceptualization.

Funding

The support for this work was provided by the National Institute on Alcohol Abuse and Alcoholism of the National Institutes of Health under award number R01AA025337 (JB, PI). The content of this article is solely the responsibility of the authors and does not necessarily represent the official view of the National Institutes of Health. A portion of this work was performed in the McKnight Brain Institute at the National High Magnetic Field Laboratory's Advanced Magnetic Resonance Imaging and Spectroscopy (AMRIS) Facility, which is supported by National Science Foundation Cooperative Agreement DMR-1644779 and the State of Florida. This work was also supported in part by an NIH award, S10 OD021726, for High End Instrumentation.

Declaration of Competing Interest

The authors declare the following financial interests/personal

relationships which may be considered as potential competing interests: Jeff Boissoneault reports financial support was provided by National Institute on Alcohol Abuse and Alcoholism. Jeff Boissoneault reports equipment, drugs, or supplies was provided by National Science Foundation. Jeff Boissoneault reports equipment, drugs, or supplies was provided by National Institutes of Health Office of the Director. If there are other authors, they declare that they have no known competing financial interests or personal relationships that could have appeared to influence the work reported in this paper.

References

Achard, S., Bullmore, E., 2007. Efficiency and cost of economical brain functional networks. PLoS Comput. Biol. 3 (2), e17.

Aghabeigi, S., Bush, N.J., Boissoneault, J., 2024. Determinants of perceived pain relief from acute alcohol intake in a laboratory setting. Drug Alcohol Depend. Rep. 12, 100267.

Alba-Ferrara, L., et al., 2016. Brain responses to emotional salience and reward in alcohol use disorder. Brain Imaging Behav. 10 (1), 136–146.

Anderson, B.M., et al., 2011. Functional imaging of cognitive control during acute alcohol intoxication. Alcohol Clin. Exp. Res 35 (1), 156–165.

Basavarajappa, B.S., Ninan, I., Arancio, O., 2008. Acute ethanol suppresses glutamatergic neurotransmission through endocannabinoids in hippocampal neurons. J. Neurochem. 107 (4), 1001–1013.

Boissoneault, J., et al., 2020. Regional increases in brain signal variability are associated with pain intensity reductions following repeated eccentric exercise bouts. Eur. J. Pain. 24 (4), 818–827.

Boissoneault, J., et al., 2023. Neural and Psychosocial Mechanisms Underlying Alcohol Use and Pain Interactions: Overview of Current Evidence and Future Directions. Curr. Addict. Rep. 10 (4), 677–689.

Boissoneault, J., Stennett, B., Robinson, M.E., 2020. Acute alcohol intake alters resting state functional connectivity of nucleus accumbens with pain-related corticolimbic structures. Drug Alcohol Depend. 207, 107811.

Bullmore, E., Sporns, O., 2009. Complex brain networks: graph theoretical analysis of structural and functional systems. Nat. Rev. Neurosci. 10 (3), 186–198.

Calhoun, V.D., et al., 2004. Alcohol intoxication effects on visual perception: an fMRI study. Hum. Brain Mapp. 21 (1), 15–26.

Cushnie, A.K., et al., 2025. Insula under the influence: Alcohol-induced changes in resting state functional connectivity. Alcohol Clin. Exp. Res (Hoboken).

Ferrarini, L., et al., 2009. Hierarchical functional modularity in the resting-state human brain. Hum. Brain Mapp. 30 (7), 2220–2231.

Garcia-Ramos, C., et al., 2016. Graph theory and cognition: A complementary avenue for examining neuropsychological status in epilepsy. Epilepsy Behav. 64 (Pt B), 329–335.

Gilman, J.M., et al., 2008. Why we like to drink: a functional magnetic resonance imaging study of the rewarding and anxiolytic effects of alcohol. J. Neurosci. 28 (18), 4583–4591.

Han, B.H., et al., 2017. Demographic trends of binge alcohol use and alcohol use disorders among older adults in the United States, 2005-2014. Drug Alcohol Depend. 170, 198–207.

Han, J., et al., 2021. Acute effects of alcohol on resting-state functional connectivity in healthy young men. Addict. Behav. 115, 106786.

Han, J., Keedy, S., de Wit, H., 2023. Stimulant-like subjective effects of alcohol are not related to resting-state connectivity in healthy men. Cereb. Cortex 33 (16), 9478–9488.

Laughlin, S.B., Sejnowski, T.J., 2003. Communication in neuronal networks. Science 301 (5641), 1870–1874.

Lee, H., et al., 2023. Graph Theoretical Analysis of Brain Structural Connectivity in Patients with Alcohol Dependence. Exp. Neurobiol. 32 (5), 362–369.

Marinkovic, K., et al., 2012. Acute alcohol intoxication impairs top-down regulation of Stroop incongruity as revealed by blood oxygen level-dependent functional magnetic resonance imaging. Hum. Brain Mapp. 33 (2), 319–333.

Masuda, N., et al., 2018. Clustering coefficients for correlation networks. Front. Neuroinform. 12, 7.

McCutcheon, J.E., et al., 2012. Encoding of aversion by dopamine and the nucleus accumbens. Front Neurosci. 6, 137.

Menardi, A., Spoa, M., Vallesi, A., 2024. Brain topology underlying executive functions across the lifespan: focus on the default mode network. Front. Psychol. 15, 1441584.

Meunier, D., et al., 2009. Hierarchical modularity in human brain functional networks. Front Neuroinform. 3, 37.

Monds, L.A., et al., 2021. How intoxicated are you? Investigating self and observer intoxication ratings in relation to blood alcohol concentration. Drug Alcohol Rev. 40 (7), 1173–1177.

Morean, M.E., Corbin, W.R., Treat, T.A., 2013. The Subjective Effects of Alcohol Scale: development and psychometric evaluation of a novel assessment tool for measuring subjective response to alcohol. Psychol. Assess. 25 (3), 780–795.

Morzorati, S.L., et al., 2002. Self-reported subjective perception of intoxication reflects family history of alcoholism when breath alcohol levels are constant. Alcohol Clin. Exp. Res 26 (8), 1299–1306.

Paulus, M.P., et al., 2006. Alcohol attenuates load-related activation during a working memory task: relation to level of response to alcohol. Alcohol Clin. Exp. Res 30 (8), 1363–1371.

Radicchi, F., et al., 2004. Defining and identifying communities in networks. Proc. Natl. Acad. Sci. USA 101 (9), 2658–2663.

Roberto, M., et al., 2003. Ethanol increases GABAergic transmission at both pre- and postsynaptic sites in rat central amygdala neurons. Proc. Natl. Acad. Sci. USA 100 (4), 2053–2058.

Roche, D.J., King, A.C., 2010. Alcohol impairment of saccadic and smooth pursuit eye movements: impact of risk factors for alcohol dependence. Psychopharmacol. (Berl.) 212 (1), 33–44.

Salinas, E., Sejnowski, T.J., 2001. Correlated neuronal activity and the flow of neural information. Nat. Rev. Neurosci. 2 (8), 539–550.

Shokri-Kojori, E., et al., 2017. Alcohol affects brain functional connectivity and its coupling with behavior: greater effects in male heavy drinkers. Mol. Psychiatry 22 (8), 1185–1195.

Sjoerds, Z., et al., 2017. Loss of brain graph network efficiency in alcohol dependence. Addict. Biol. 22 (2), 523–534.

Sporns, O., 2018. Graph theory methods: applications in brain networks. Dialog. Clin. Neurosci. 20 (2), 111–121.

Sporns, O., Betzel, R.F., 2016. Modular Brain Networks. Annu Rev. Psychol. 67, 613–640.

Stennett-Blackmon, B.A., Sevel, L., Boissoneault, J., 2023. Association of cerebellar and pre-motor cortex gray matter density with subjective intoxication and subjective response following acute alcohol intake. Sci. Rep. 13 (1), 7340.

Visontay, R., et al., 2022. Are there non-linear relationships between alcohol consumption and long-term health?: a systematic review of observational studies employing approaches to improve causal inference. BMC Med Res Method. 22 (1), 16.

Volkow, N.D., et al., 1988. Effects of acute alcohol intoxication on cerebral blood flow measured with PET. Psychiatry Res. 24 (2), 201–209.

Wang, B., LeBel, A., D'Mello, A.M., 2025. Ignoring the cerebellum is hindering progress in neuroscience. Trends Cogn. Sci. 29 (4), 318–330.

Watts, D.J., Strogatz, S.H., 1998. Collective dynamics of 'small-world' networks. Nature 393 (6684), 440–442.

Yeung, H.W., et al., 2021. Spectral clustering based on structural magnetic resonance imaging and its relationship with major depressive disorder and cognitive ability. Eur. J. Neurosci. 54 (6), 6281–6303.

You, C., Vandegrift, B., Brodie, M.S., 2018. Ethanol actions on the ventral tegmental area: novel potential targets on reward pathway neurons. Psychopharmacology 235 (6), 1711–1726.

Z.W, C., 1940. The Effect of alcohol on vision: an experimental investigation. JAMA Netw. 115 (18), 1525–1527.

Zhang, G., et al., 2022. Analysis on topological alterations of functional brain networks after acute alcohol intake using resting-state functional magnetic resonance imaging and graph theory. Front Hum. Neurosci. 16, 985986.